

Synthesis and characterization of $\text{LiCo}_x\text{Mn}_y\text{Ni}_{1-x-y}\text{O}_2$ as a cathode material for secondary lithium batteries

Yao Chen^{*}, G.X. Wang, K. Konstantinov, H.K. Liu, S.X. Dou

Institute for Superconducting & Electronic Materials, University of Wollongong, Wollongong, NSW 2522, Australia

Abstract

The synthesis and electrochemical characteristics of $\text{LiCo}_x\text{Mn}_y\text{Ni}_{1-x-y}\text{O}_2$ as cathode materials for rechargeable lithium-ion batteries were investigated. The precursor $\text{Co}_x\text{Mn}_y\text{Ni}_{1-x-y}(\text{OH})_2$ was obtained by the chemical co-precipitation method. $\text{LiCo}_x\text{Mn}_y\text{Ni}_{1-x-y}\text{O}_2$ ($0 \leq x \leq 0.3$, and $y = 0.2$) was prepared by heating a mixture of $\text{Co}_x\text{Mn}_y\text{Ni}_{1-x-y}(\text{OH})_2$ and Li_2CO_3 at 850–900 °C for 24 h in air. The X-ray diffraction (XRD) patterns indicated that pure phase $\text{LiCo}_x\text{Mn}_y\text{Ni}_{1-x-y}\text{O}_2$ was obtained. The scanning electron micrographs (SEMs) show that the synthesized $\text{LiCo}_x\text{Mn}_y\text{Ni}_{1-x-y}\text{O}_2$ compounds have good micro-morphology and uniform particle size. The electrochemical properties of these materials such as the galvanostatic charge–discharge performance and cyclic voltammetry were systematically measured.

© 2003 Elsevier Science B.V. All rights reserved.

Keywords: Cathode material; Lithium-ion batteries; Co-precipitation; $\text{Co}_x\text{Mn}_y\text{Ni}_{1-x-y}(\text{OH})_2$; $\text{LiCo}_x\text{Mn}_y\text{Ni}_{1-x-y}\text{O}_2$

1. Introduction

Rechargeable lithium-ion batteries are becoming increasingly important as power sources for portable consumer electronics. LiCoO_2 has been widely used as a cathode material in commercial lithium-ion battery production because it is reasonably easy to synthesize and shows a stable discharge capacity. However, due to the high cost and toxicity of LiCoO_2 , many efforts have been made to replace it. LiNiO_2 is an attractive material because of its low cost and its possibility of offering a high charge–discharge capacity. The two major problems for LiNiO_2 are the difficulty in attaining the correct stoichiometry and the poor cycle life. In an attempt to overcome these problems, a great deal of effort has been concentrated on doped materials that may possess properties superior to pure LiNiO_2 . A series of $\text{LiCo}_x\text{Ni}_{1-x}\text{O}_2$ compounds has been studied [1–5]. Zhecheva and Stoyanova [2] have shown that cobalt substitution sharply decreases the non-stoichiometry of lithium nickel oxide and thus stabilizes the alternating layered structure. Although high cobalt doping ($x \geq 0.3$) is reported to be necessary for obtaining better electrochemical performance, the replacement of Ni by the more expensive Co also adds to

the cost of material synthesis at the same time. There are thus attempts to partially replace Ni in LiNiO_2 by low cost Mn [6–8]. The research results have shown that the capacity fading of $\text{LiMn}_x\text{Ni}_{1-x}\text{O}_2$ is lower than for LiNiO_2 but its overall capacity is also decreased. To overcome the relatively lower capacity of $\text{LiMn}_x\text{Ni}_{1-x}\text{O}_2$, an additional low doping with Co (≤ 0.3) is used in $\text{LiMn}_x\text{Ni}_{1-x}\text{O}_2$ because the presence of cobalt stabilizes the structure [9,10]. Ohzuku et al. [10] and Yoshio et al. [8] studied respectively the preparation of single-phase $\text{LiCo}_{1/3}\text{Mn}_{1/3}\text{Ni}_{1/3}\text{O}_2$ and $\text{LiCo}_x\text{Mn}_y\text{Ni}_{1-x-y}\text{O}_2$ ($x \leq 0.3$, $y = 0.2$) by using the solid-state solution method. In this paper, we report on the synthesis of $\text{LiCo}_x\text{Mn}_y\text{Ni}_{1-x-y}\text{O}_2$ ($x \leq 0.2$, $y = 0.2$) by using $\text{Co}_x\text{Mn}_y\text{Ni}_{1-x-y}(\text{OH})_2$ precursor and Li_2CO_3 as the starting materials (Fig. 1). The resulting compounds demonstrated good battery performance.

2. Experimental

$\text{Co}(\text{NO}_3)_2 \cdot 6\text{H}_2\text{O}$ (>98%, Aldrich), $\text{Ni}(\text{NO}_3)_2 \cdot 6\text{H}_2\text{O}$ (>98%, Aldrich) and $(\text{CH}_3\text{CO}_2)_2\text{Mn} \cdot 6\text{H}_2\text{O}$ were used as the starting materials and were dissolved in distilled water in stoichiometric amounts. The solution was slowly dripped into a 50 ml aqueous solution that was maintained at 60 °C under rapid stirring. At the same time, a NaOH (6 M) and NH_3OH (6.5 M) solution mixture was slowly pumped into the solution by a

^{*} Corresponding author. Tel.: +61-2-4221-5615; fax: +61-2-4221-5731.
E-mail address: yao_chen@uow.edu.au (Y. Chen).

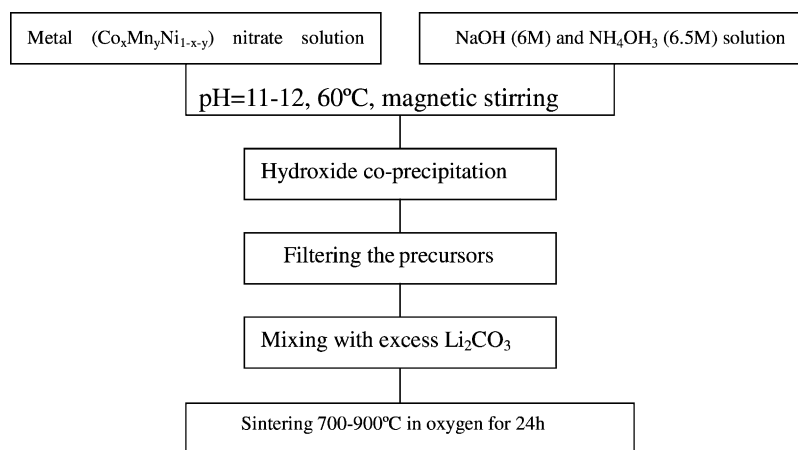


Fig. 1. Flow-chart of the synthesis procedure.

peristaltic pump to maintain the pH value of the solution at $\text{pH} = 11\text{--}12$. The mixed hydroxide co-precipitate thus obtained was first filtered and thoroughly washed with distilled water, then dried at 65°C overnight, giving the precursor precipitate $(\text{Co}_x\text{Mn}_y\text{Ni}_{1-x-y})(\text{OH})_2$. The precursor and Li_2CO_3 were mixed and ground using a mortar and pestle. The mixture was then pressed into pellets (20 mm diameter and 5 mm thick) at 800 kg/cm^2 . The disks obtained were heated in air at $700\text{--}900^\circ\text{C}$ for 24 h. Three $\text{LiCo}_x\text{Mn}_y\text{Ni}_{1-x-y}\text{O}_2$ compounds were prepared, which are $\text{LiCo}_{0.05}\text{Mn}_{0.2}\text{Ni}_{0.75}\text{O}_2$, $\text{LiCo}_{0.1}\text{Mn}_{0.2}\text{Ni}_{0.7}\text{O}_2$ and $\text{LiCo}_{0.2}\text{Mn}_{0.2}\text{Ni}_{0.6}\text{O}_2$.

The structure of the $\text{LiCo}_x\text{Mn}_y\text{Ni}_{1-x-y}\text{O}_2$ was characterized by X-ray diffraction (XRD) ($\text{MO}_3\cdot x\text{HF}_{22}$, MacScience Co. Ltd., Japan) using $\text{Cu K}\alpha$ radiation. The morphology of the $\text{LiCo}_x\text{Mn}_y\text{Ni}_{1-x-y}\text{O}_2$ powders was observed by using scanning electron micrograph (SEM) (Leica/Cambridge Steroscan 440 scanning electron microscope).

The charge–discharge characteristics of the $\text{LiCo}_x\text{Mn}_y\text{Ni}_{1-x-y}\text{O}_2$ cathodes were examined in Teflon testing cells. The electrodes were made by dispersing 85 wt.% active materials, 13 wt.% carbon black and 2 wt.% polyvinylidene fluoride (PVDF) binder in dimethyl phthalate solvent to form a slurry, which was then spread onto a piece of aluminum foil and dried in oven overnight at 95°C . The thickness of the electrode was approximately $50\text{--}60\ \mu\text{m}$ with a loading of $1\text{--}2\text{ mg}$ active material per electrode. The cell was comprised of a cathode and lithium metal anode separated by a polypropylene separator and was assembled in an argon filled glove-box (Mbraun, Unilab, USA). The electrolyte was 1 M LiPF_6 in a mixture of ethylene carbonate (EC) and dimethyl carbonate (DMC) (1:1 by volume, provided by Merck KgaA, Germany). The cells were cycled between 3.0 and 4.3 V versus Li/Li^+ at room temperature to measure the electrochemical response. Cyclic voltammetry (CV) was performed to determine the characteristics of the lithium reaction with cathode electrodes. The CV measurements were carried out on a potentiostat (Model M362, EG&G Princeton Applied Research, USA) at a scanning rate of 1 mV/s .

3. Results and discussion

3.1. Physical characterization of $\text{LiCo}_x\text{Mn}_y\text{Ni}_{1-x-y}\text{O}_2$

X-ray and SEM observation were used to characterize the $\text{LiCo}_x\text{Mn}_y\text{Ni}_{1-x-y}\text{O}_2$ powders. Fig. 2(a) shows typical XRD

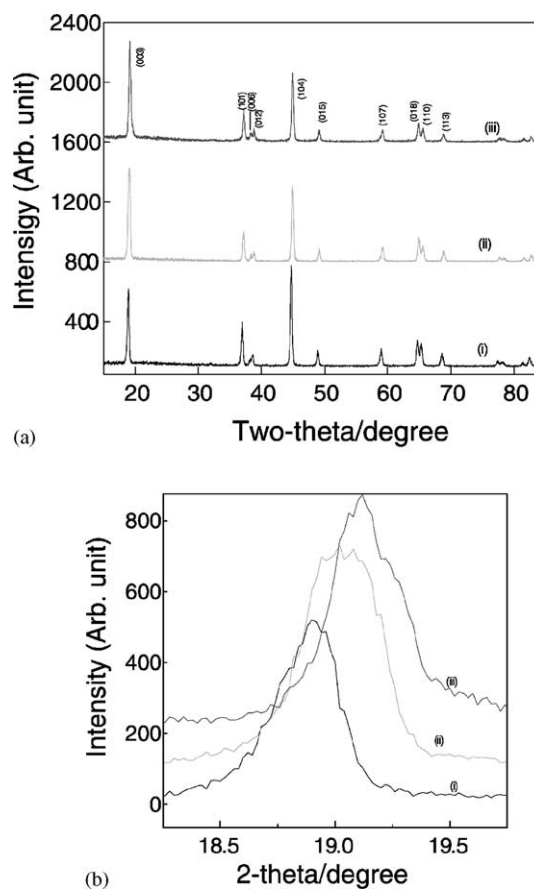


Fig. 2. (a) XRD patterns for (i) $\text{LiCo}_{0.05}\text{Mn}_{0.2}\text{Ni}_{0.75}\text{O}_2$; (ii) $\text{LiCo}_{0.1}\text{Mn}_{0.2}\text{Ni}_{0.7}\text{O}_2$; (iii) $\text{LiCo}_{0.2}\text{Mn}_{0.2}\text{Ni}_{0.6}\text{O}_2$. (b) Enlarged (0 0 3) peaks of (i) $\text{LiCo}_{0.05}\text{Mn}_{0.2}\text{Ni}_{0.75}\text{O}_2$; (ii) $\text{LiCo}_{0.1}\text{Mn}_{0.2}\text{Ni}_{0.7}\text{O}_2$; (iii) $\text{LiCo}_{0.2}\text{Mn}_{0.2}\text{Ni}_{0.6}\text{O}_2$.

Table 1

Lattice parameters and volume of the $\text{LiCo}_x\text{Mn}_y\text{Ni}_{1-x-y}\text{O}_2$ unit cell and intensity ratio $I(0\ 0\ 3)/I(1\ 0\ 4)$

Composition	a (Å)	c (Å)	Volume (Å ³)	Intensity ratio of $I(0\ 0\ 3)/I(1\ 0\ 4)$
$\text{LiCo}_{0.05}\text{Mn}_{0.2}\text{Ni}_{0.75}\text{O}_2$	2.8536	14.1540	99.7363	1.40
$\text{LiCo}_{0.1}\text{Mn}_{0.2}\text{Ni}_{0.7}\text{O}_2$	2.8516	14.1426	99.5138	1.20
$\text{LiCo}_{0.2}\text{Mn}_{0.2}\text{Ni}_{0.6}\text{O}_2$	2.8479	14.1313	99.4154	0.77

patterns of $\text{LiCo}_x\text{Mn}_y\text{Ni}_{1-x-y}\text{O}_2$. A pure phase of $\text{LiCo}_x\text{Mn}_y\text{Ni}_{1-x-y}\text{O}_2$ could be identified. All of the peaks can be indexed based on a hexagonal $\alpha\text{-NaFeO}_2$ structure in which the transition metal ions are surrounded by six oxygen atoms. Fig. 2(b) (enlarged (0 0 3) peak) shows that the (0 0 3) peak of $\text{LiCo}_x\text{Ni}_{1-x}\text{O}_2$ shifts with the Co doping level. Table 1 gives the computed results of the lattice parameters of the hexagonal cell and the intensity ratio $I(0\ 0\ 3)/I(1\ 0\ 4)$. The value of the parameters and their increasing evolution with cobalt content is in agreement with results reported in the literature for lithium–nickel–cobalt compounds [10–12]. The lattice parameters, a , c , and volume decreased when the cobalt content increased. The unit cell dimensions in a hexagonal setting shrink with an increase in the Co doping level as was the case for $\text{LiCo}_x\text{Ni}_{1-x}\text{O}_2$ because of the difference in size between trivalent cobalt and trivalent nickel ions ($r_{\text{Ni}^{3+}} = 0.56$ Å and $r_{\text{Co}^{3+}} = 0.53$ Å) [11]. These data show that with an increase in Co content the non-stoichiometry diminishes while the order of the structure becomes higher. The ratio of $I(0\ 0\ 3)/I(1\ 0\ 4)$ is increased with an increasing Co doping level. The intensity ratio has been reported to be closely related to undesirable cation mixing, which is reduced as the value of the ratio is increased [12].

SEMs of $\text{LiCo}_x\text{Mn}_y\text{Ni}_{1-x-y}\text{O}_2$ powders are similar (Fig. 3). The powders consist of cubic grains with a size in the range of 0.1–5 μm together with larger agglomerates.

3.2. Electrochemical characteristics of $\text{LiCo}_x\text{Mn}_y\text{Ni}_{1-x-y}\text{O}_2$

Cyclic voltammetry measurements were performed on $\text{LiCo}_{0.05}\text{Mn}_{0.2}\text{Ni}_{0.75}\text{O}_2$ and $\text{LiCo}_{0.2}\text{Mn}_{0.2}\text{Ni}_{0.6}\text{O}_2$ electrodes at a sweep rate of 0.1 mV/s over a voltage of 3.0–4.5 V. Fig. 4(a) and 4(b) shows the cyclic voltammograms of $\text{LiCo}_{0.2}\text{Mn}_{0.2}\text{Ni}_{0.6}\text{O}_2$ and $\text{LiCo}_{0.05}\text{Mn}_{0.2}\text{Ni}_{0.75}\text{O}_2$, respectively. It can be seen that the two materials both have a similar well-defined peak representing the de-intercalation of Li^+ from the initial structure that is observed in a narrow potential range. This implies that the extraction of Li^+ occurs easily from an ordered and stabilized layered structure. In the case of $\text{LiCo}_{0.05}\text{Mn}_{0.2}\text{Ni}_{0.75}\text{O}_2$, the main oxidation peak is observed at 3.93 V, while the main reduction peak appears at 3.74 V. For $\text{LiCo}_{0.2}\text{Mn}_{0.2}\text{Ni}_{0.6}\text{O}_2$, these peaks appeared at potentials close to 3.88 and 3.73 V, respectively. The difference between the cathode and anode peak of $\text{LiCo}_{0.2}\text{Mn}_{0.2}\text{Ni}_{0.6}\text{O}_2$ is less than for $\text{LiCo}_{0.05}\text{Mn}_{0.2}\text{Ni}_{0.75}\text{O}_2$. At the same

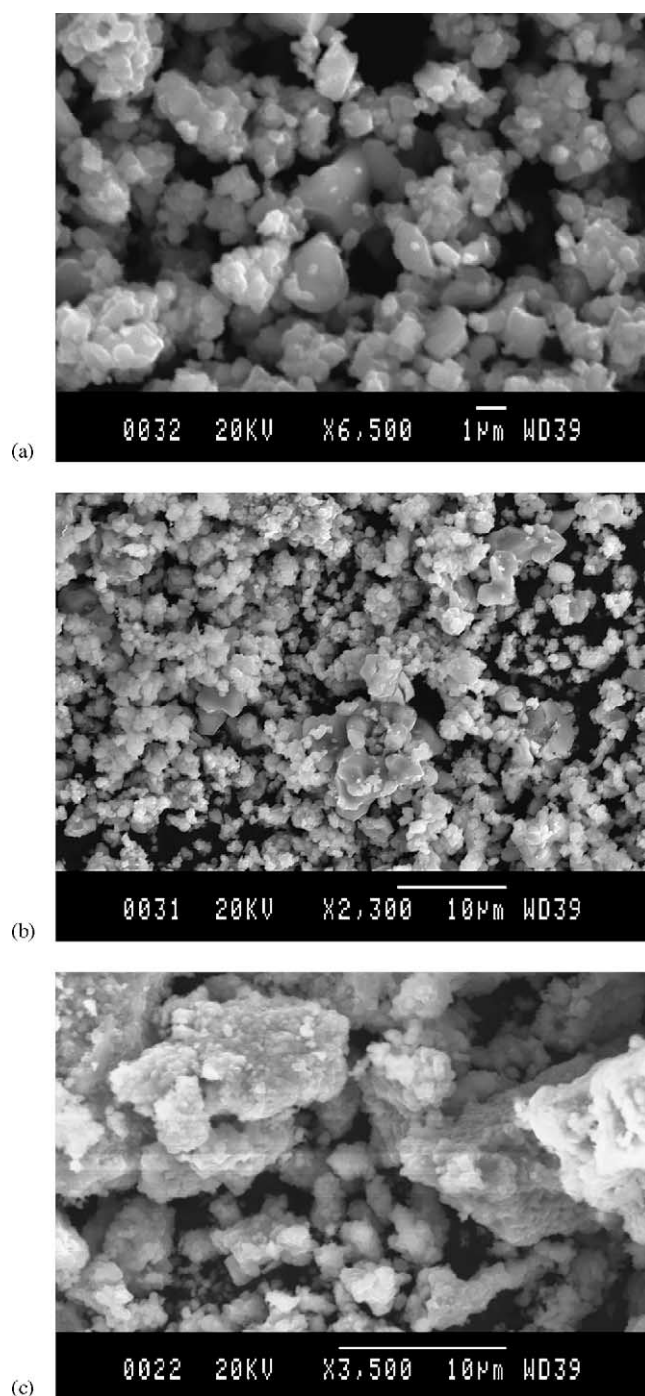


Fig. 3. SEM micrographs of $\text{LiCo}_x\text{Mn}_y\text{Ni}_{1-x-y}\text{O}_2$ cathodes: (a) $\text{LiCo}_{0.05}\text{Mn}_{0.2}\text{Ni}_{0.75}\text{O}_2$; (b) $\text{LiCo}_{0.1}\text{Mn}_{0.2}\text{Ni}_{0.7}\text{O}_2$; (c) $\text{LiCo}_{0.2}\text{Mn}_{0.2}\text{Ni}_{0.6}\text{O}_2$.

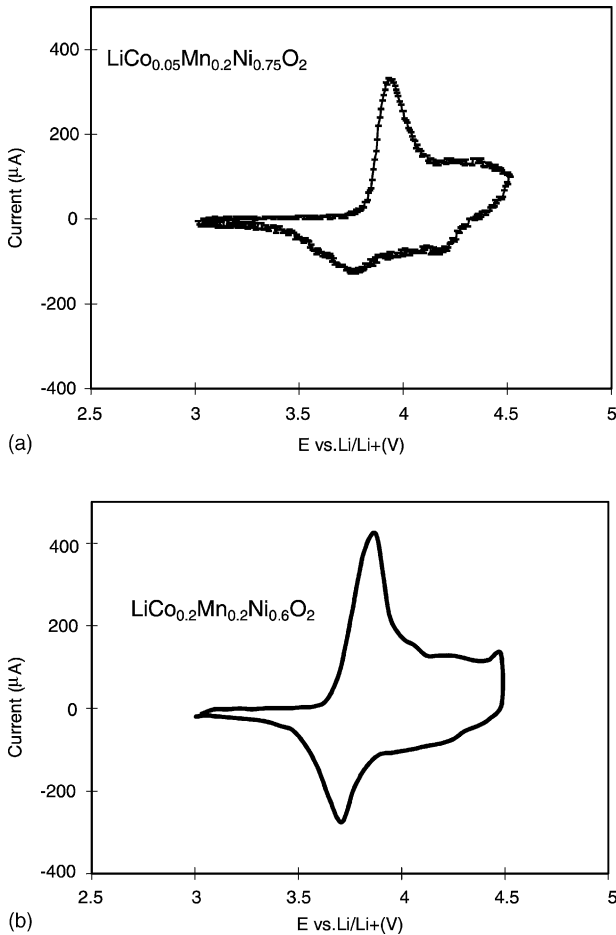


Fig. 4. (a) Cyclic voltammograms of $\text{LiCo}_{0.05}\text{Mn}_{0.2}\text{Ni}_{0.75}\text{O}_2$; (b) cyclic voltammograms of $\text{LiCo}_{0.2}\text{Mn}_{0.2}\text{Ni}_{0.6}\text{O}_2$.

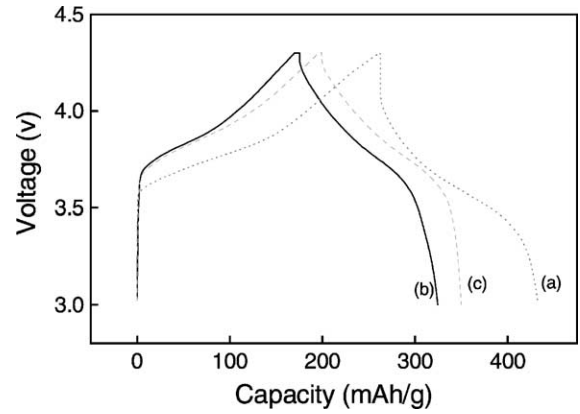


Fig. 5. The initial charge–discharge curves of $\text{LiCo}_x\text{Mn}_y\text{Ni}_{1-x-y}\text{O}_2$: (a) $\text{LiCo}_{0.05}\text{Mn}_{0.2}\text{Ni}_{0.75}\text{O}_2$; (b) $\text{LiCo}_{0.1}\text{Mn}_{0.2}\text{Ni}_{0.7}\text{O}_2$; (c) $\text{LiCo}_{0.2}\text{Mn}_{0.2}\text{Ni}_{0.6}\text{O}_2$.

time, the reduction peak of the former is much better than in the case of 0.05 Co^{3+} . It is clear that the reversibility of $\text{LiCo}_{0.2}\text{Mn}_{0.2}\text{Ni}_{0.6}\text{O}_2$ is larger than for $\text{LiCo}_{0.05}\text{Mn}_{0.2}\text{Ni}_{0.75}\text{O}_2$ due to fact that enhanced stability and structural order increase with the Co content. In Fig. 4(a), two reduction peaks at 3.74 V and 4.16 V are observed in the discharge process. The reduction peak at 4.16 V is possibly associated with the participation of Mn in lithiation reactions.

$\text{LiCo}_x\text{Mn}_y\text{Ni}_{1-x-y}\text{O}_2$ ($x = 0.05, 0.1, \text{ and } 0.2, y = 0.2$) electrodes were cycled in the voltage window of 3.0–4.3 V at a current density of 0.4 mA/cm^2 at room temperature. Fig. 5 shows the initial charge–discharge profiles. The charge and discharge capacities of $\text{LiCo}_{0.1}\text{Mn}_{0.2}\text{Ni}_{0.7}\text{O}_2$ and $\text{LiCo}_{0.2}\text{Mn}_{0.2}\text{Ni}_{0.6}\text{O}_2$ were smaller than for $\text{LiCo}_{0.05}\text{Mn}_{0.2}\text{Ni}_{0.75}\text{O}_2$ due to the Co doping level. However, it can also be

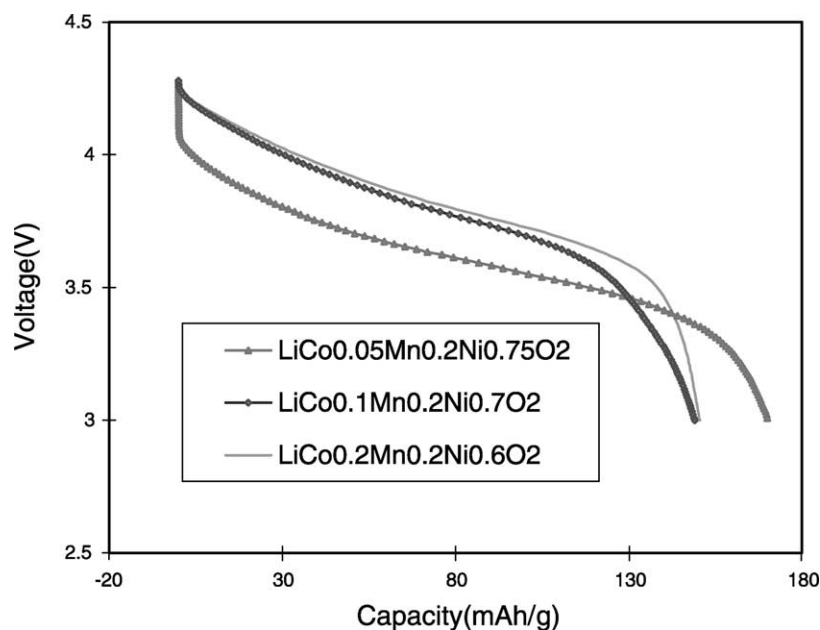


Fig. 6. The initial discharge curves of $\text{LiCo}_x\text{Mn}_y\text{Ni}_{1-x-y}\text{O}_2$.

determined from this figure that the irreversible capacity of $\text{LiCo}_{0.05}\text{Mn}_{0.2}\text{Ni}_{0.75}\text{O}_2$ in the first cycle is the highest among the three materials. The reversible capacity increases with Co content as is proved by the cyclic voltammetry curve. The discharge capacities of $\text{LiCo}_{0.1}\text{Mn}_{0.2}\text{Ni}_{0.7}\text{O}_2$ and $\text{LiCo}_{0.2}\text{Mn}_{0.2}\text{Ni}_{0.6}\text{O}_2$ were very similar because of these two effects of Co doping [10]. Fig. 6 shows that the three materials have large initial discharge capacities of 150–170 mAh/g. The initial discharge capacity of $\text{LiCo}_{0.05}\text{Mn}_{0.2}\text{Ni}_{0.75}\text{O}_2$ is highest but it has a lower (average) discharge potential compared to the two other materials due to its high Ni content. The discharge potentials increase with increasing Co doping level. $\text{LiCo}_{0.2}\text{Mn}_{0.2}\text{Ni}_{0.6}\text{O}_2$ demonstrated the highest discharge potential. However, the discharge capacities of $\text{LiCo}_{0.1}\text{Mn}_{0.2}\text{Ni}_{0.7}\text{O}_2$ and $\text{LiCo}_{0.2}\text{Mn}_{0.2}\text{Ni}_{0.6}\text{O}_2$ were similar.

It should be noted that the electrochemical performances of our samples are as good as what has been reported for samples made by the solid-state solution method [9,10].

4. Conclusion

Single-phase electroactive $\text{LiCo}_x\text{Mn}_y\text{Ni}_{1-x-y}\text{O}_2$ compounds were obtained from lithium compounds and the precursor $\text{Co}_x\text{Mn}_y\text{Ni}_{1-x-y}(\text{OH})_2$ by heating in air at 850–

900 °C. The synthesized $\text{LiCo}_x\text{Mn}_y\text{Ni}_{1-x-y}\text{O}_2$ has good morphology and uniform particle size. $\text{LiCo}_{0.1}\text{Mn}_{0.2}\text{Ni}_{0.7}\text{O}_2$ and $\text{LiCo}_{0.2}\text{Mn}_{0.2}\text{Ni}_{0.6}\text{O}_2$ had the best electrochemical characteristics among the three materials and their initial discharge capacities attained 150 mAh/g.

References

- [1] T. Ohzuku, A. Ueda, M. Nagayama, Y. Iwakoshi, H. Komori, *Electrochim. Acta* 38 (1993) 1159.
- [2] E. Zhecheva, R. Stoyanova, *Solid State Ionics* 66 (1993) 143.
- [3] D. Caurant, N. Baffier, B. Garcia, J.P. Pereira-Ramos, *Solid State Ionics* 91 (1996) 45.
- [4] B. Banov, J. Bourikov, M. Mladenov, *J. Power Sources* 54 (1995) 268.
- [5] C. Nayoze, F. Ansart, C. Laberty, J. Sarrias, A. Rousset, *J. Power Sources* 99 (2001) 54.
- [6] Y. Nitta, K. Okamura, K. Haraguchi, S. Kobayashi, A. Ohta, *J. Power Sources* 54 (1995) 511.
- [7] E. Rossen, C.D.W. Jones, J.R. Dahn, *Solid State Ionics* 57 (1992) 311.
- [8] M. Yoshio, Y. Todorov, K. Yamato, *J. Power Sources* 74 (1998) 46.
- [9] T. Ohzuku, Y. Makimura, *Chem. Lett.* (2001) 642.
- [10] M. Yoshio, H. Noguchi, J. Itoh, M. Okada, T. Mouri, *J. Power Sources* 90 (2000) 176.
- [11] R.D. Shannon, G.T. Prewitt, *Acta Crystallogr., Sect. B* 25 (1969) 925.
- [12] C. Delmas, I. Saadoune, A. Rougier, *J. Power Sources* 89 (1996) 43.